Genome-wide bimolecular fluorescence complementation analysis of SUMO interactome in yeast

Min-Kyung Sung,[1,2] Gyubum Lim,[1,2] Dae-Gwan Yi,[1,2] Yeon Ji Chang,[1,2] Eun Bin Yang,[1] KiYoung Lee,[3] and Won-Ki Huh[1,2,4]

[1]*Department of Biological Sciences, Seoul National University, Seoul 151-747, Republic of Korea;* [2]*Research Center for Functional Cellulomics and Institute of Microbiology, Seoul National University, Seoul 151-742, Republic of Korea;* [3]*Department of Biomedical Informatics, Ajou University School of Medicine, Suwon 443-749, Republic of Korea*

The definition of protein–protein interactions (PPIs) in the natural cellular context is essential for properly understanding various biological processes. So far, however, most large-scale PPI analyses have not been performed in the natural cellular context. Here, we describe the construction of a *Saccharomyces cerevisiae* fusion library in which each endogenous gene is C-terminally tagged with the N-terminal fragment of Venus (VN) for a genome-wide bimolecular fluorescence complementation assay, a powerful technique for identifying PPIs in living cells. We illustrate the utility of the VN fusion library by systematically analyzing the interactome of the small ubiquitin-related modifier (SUMO) and provide previously unavailable information on the subcellular localization, types, and protease dependence of SUMO interactions. Our data set is highly complementary to the existing data sets and represents a useful resource for expanding the understanding of the physiological roles of SUMO. In addition, the VN fusion library provides a useful research tool that makes it feasible to systematically analyze PPIs in the natural cellular context.

[Supplemental material is available for this article.]

Most biological processes are mediated by complicated networks of protein–protein interactions (PPIs). Thus, the identification of the occurrence and components of PPIs provides invaluable insights into the cellular functions of proteins. In addition to conventional coimmunoprecipitation techniques, several methods have been developed to study PPIs, including the yeast two-hybrid analysis (Fields and Song 1989), the split ubiquitin system (Johnsson and Varshavsky 1994), fluorescence resonance energy transfer (FRET) assays (Periasamy and Day 1999; Pollok and Heim 1999), tandem affinity purification (TAP) followed by mass spectrometry (MS) analysis (Rigaut et al. 1999), and protein fragment complementation (PFC) assays (Remy and Michnick 1999; Ghosh et al. 2000; Wehrman et al. 2002; Paulmurugan and Gambhir 2003). Recently, the bimolecular fluorescence complementation (BiFC) assay, a specialized form of the PFC assay that uses fluorescent proteins as a reporter, has been developed (Hu et al. 2002). The BiFC assay is based on the formation of a fluorescent complex when two proteins fused to nonfluorescent fragments of a fluorescent protein interact with each other. This approach enables direct visualization of the occurrence and subcellular localization of PPIs with simple equipment.

The budding yeast *Saccharomyces cerevisiae* has been a valuable eukaryotic model system, not only for traditional molecular and cell biology but also for the fields of functional genomics and proteomics. In *S. cerevisiae*, several large-scale analyses of PPIs have been performed with the yeast two-hybrid method (Uetz et al. 2000; Ito et al. 2001) or TAP-MS analysis (Gavin et al. 2002, 2006; Ho et al. 2002; Krogan et al. 2006). However, these approaches do not measure PPI in the natural cellular context; the yeast two-hybrid method is not appropriate for analyzing the interactions between proteins that cannot be transported to the nucleus or that form interactions only in the presence of other stabilizing interactions, and TAP-MS analysis is not amenable to studying protein complexes that are weakly or transiently formed or that do not survive in vitro purification. Compared with the yeast two-hybrid method and TAP-MS analysis, the FRET, PFC, and BiFC assays have several advantages in that they can detect the interactions between proteins in their natural cellular environment. Recently, a large-scale PPI screen using the PFC assay based on reconstituted dihydrofolate reductase (DHFR) activity has been reported (Tarassov et al. 2008), which is the first example of genome-wide PPI analysis using the PFC assay. However, because positive PPIs are selected by methotrexate resistance in the DHFR PFC assay, it is possible that the addition of methotrexate to the assay medium may perturb cellular physiology and proper PPI networks. In this regard, large-scale PPI screens using the BiFC or FRET assay that do not require any exogenous reagents would provide more accurate information about the structural organization of PPI networks in cells. To date, however, there is no report describing the application of the BiFC or FRET assay to genome-wide PPI analyses, particularly using proteins expressed from their own native promoters.

The small ubiquitin-related modifier (SUMO) proteins are ~10 kDa in size and comprise a family of evolutionarily conserved polypeptides that are post-translationally attached to the lysine residues of target proteins to regulate their subcellular localization, stability, and activity (Kerscher et al. 2006; Geiss-Friedlander and Melchior 2007). SUMO conjugation plays a variety of important roles in diverse eukaryotic cellular processes. SUMO can also mediate the non-covalent interaction of substrate proteins with proteins containing SUMO-interacting motifs and modulate their function (Song et al. 2004). In this regard, the identification of

[4]Corresponding author
E-mail wkh@snu.ac.kr
Article published online before print. Article, supplemental material, and publication date are at http://www.genome.org/cgi/doi/10.1101/gr.148346.112.

23:736–746 © 2013, Published by Cold Spring Harbor Laboratory Press; ISSN 1088-9051/13; www.genome.org

SUMO target proteins is crucial for the elucidation of the function of SUMO. Recent genome-wide PPI screens have identified over 500 putative SUMO conjugates in *S. cerevisiae* (Panse et al. 2004; Wohlschlegel et al. 2004; Zhou et al. 2004; Denison et al. 2005; Hannich et al. 2005; Wykoff and O'Shea 2005). More recently, an elegant study integrating the information of PPIs and genetic interactions has been conducted and has uncovered novel functional relationships between the SUMO pathway and various biological processes (Makhnevych et al. 2009). These systematic analyses have expanded the pool of SUMO substrates and the understanding of the biological function of sumoylation. However, because SUMO substrates can undergo rapid cycles of modification and demodification, and most target proteins appear to be modified to a small percentage at steady state (Geiss-Friedlander and Melchior 2007), it is likely that many unknown SUMO substrates remain to be discovered. Moreover, previous systematic PPI screens to identify SUMO substrates have primarily been performed with the yeast two-hybrid method and TAP-MS, which do not measure PPIs in the natural cellular context. The low agreement between the data from previous systematic screens demonstrates the limitation of the experimental methods used in those analyses and indicates that no single screen has been comprehensive. For this reason, different systematic approaches, with methods that can detect the interactions between proteins in their natural cellular environment, would greatly contribute to the identification of novel SUMO substrates and thus to the understanding of the function of the SUMO pathway.

In the present study, we generated a collection of yeast strains expressing full-length proteins tagged with the N-terminal fragment of Venus (VN), a yellow fluorescent protein variant, from their own native promoters. Through a systematic analysis with the VN fusion library, we identified the interactome of SUMO, comprising 367 proteins, and also obtained previously unavailable information on the subcellular localization, types, and protease dependence of SUMO interactions in living yeast cells. Our data not only highlight a novel relationship between sumoylation and various biological processes but also represent a valuable resource that can be used to study the functional roles of the SUMO pathway. This is the first report that describes the application of the BiFC assay to a genome-wide PPI analysis using proteins expressed from their own native promoters. As demonstrated here, the VN fusion library provides a useful research tool that makes it feasible to systematically analyze PPIs in the natural cellular context.

Results

Construction and utilization of the VN fusion library

To facilitate the application of the BiFC assay to the genome-wide analysis of PPIs, we attempted to construct a *S. cerevisiae* fusion library in which each endogenous gene is C-terminally tagged with VN so that each fusion protein can be expressed from its own native promoter. First, we generated the pFA6a-VN-KlURA3 vector for switching C-terminally tagged epitopes to the VN tag (Fig. 1A), based on an epitope switching strategy (Sung et al. 2008). A DNA fragment containing the VN tag and *KlURA3* marker sequences was amplified by PCR with pFA6a-VN-KlURA3 as the template and the set of universal primers F2CORE and R1CORE (Fig. 1A; Supplemental Table S1). The resulting PCR products were transformed into each strain of the TAP fusion library (Ghaemmaghami et al. 2003), which consists of 6097 *MAT***a** strains with chromosomal C-terminally TAP-tagged open reading frames (ORFs) that encompass 98% of all ORFs annotated in the *Saccharomyces* genome database (as of April 2001; http://www.yeastgenome.org). Transformants were subjected to medium selection and counter-selection to verify that the VN tag was successfully switched from the TAP tag at the corresponding locus (Fig. 1B, left panel). Immunoblotting of some of the transformants that passed medium selection/counter-selection further confirmed successful switching from the TAP tag to the VN tag (Fig. 1B, right panel; Supplemental Fig. S1). Finally, we obtained 5911 VN-tagged strains with a coverage of 95% of all ORFs.

The BiFC assay with the VN fusion library provides a simple and direct means for the analysis of in vivo PPIs at a genome-wide scale. Briefly, all VN-tagged strains are mated individually with a *MAT*α strain expressing a protein of interest tagged with the C-terminal fragment of Venus (VC), thus generating 5911 diploid strains expressing both the VN fusion and the VC fusion (Fig. 1C). The resulting diploid cells are analyzed for fluorescence from the BiFC complex formation. Positive BiFC signals provide information about not only the occurrence but also the subcellular localization of PPIs. Furthermore, the evaluation of the BiFC signal intensity facilitates the quantitative analysis of condition-specific PPIs without disrupting cellular integrity, as shown previously (Sung and Huh 2010).

Identification of the SUMO interactome

Because protein sumoylation plays important roles in the regulation of various biological processes, defining the target proteins modified by or interacting with SUMO is crucial for understanding the regulatory functions of the SUMO pathway. To address this issue, we set out to identify SUMO substrates by a genome-wide BiFC assay. Previously, it has been shown that the BiFC assay can be used to detect protein sumoylation in living cells (Fang and Kerppola 2004; Sung and Huh 2010). We first constructed a *MAT*α strain expressing VC-tagged SUMO (Smt3 in *S. cerevisiae*). Because SUMO is proteolytically processed to expose the C-terminal Gly-Gly residues and the protein sumoylation patterns in cells overexpressing Smt3 differ significantly from those in wild-type cells (Wohlschlegel et al. 2004), we tagged VC at the N terminus of Smt3 and allowed VC-Smt3 to be expressed under the control of the *CET1* promoter, which is similar in strength to the *SMT3* promoter (Ghaemmaghami et al. 2003). HY1121 cells with N-terminally VC-tagged Smt3 exhibited little, if any, difference in growth (Supplemental Fig. S2A) or in the protein sumoylation pattern compared with untagged control cells (Supplemental Fig. S2B), indicating that the biological function of Smt3 is not disturbed by VC tagging. To perform a genome-wide BiFC screen for the SUMO interactome, we mated the HY1121 strain expressing VC-tagged Smt3 with each strain of the VN fusion library and analyzed the resulting diploid strains by fluorescence microscopy. Of 5911 strains examined, 408 exhibited BiFC signals above background level with a broad range of subcellular localizations (Fig. 2A; Supplemental Table S2). To determine false-positive BiFC signals arising from self-assembly of VN and VC, we generated *MAT*α strains (HY1123 and HY1125) expressing VC with or without fusion to Smt3 and mated these strains with each of the 408 VN-tagged strains identified above. The fluorescence of the resulting diploid strains was evaluated to determine whether the fluorescence intensity of cells with VC alone (F_{VC}) is comparable to that of cells with VC-Smt3 ($F_{VC\text{-}Smt3}$). Of the 408 strains, 41 exhibited $F_{VC\text{-}Smt3}/F_{VC} \leq 1$ and were regarded as false positives (Fig. 2B; Supplemental Fig. S3, gray). By excluding these 41 proteins, we finally identified 367 proteins as the SUMO

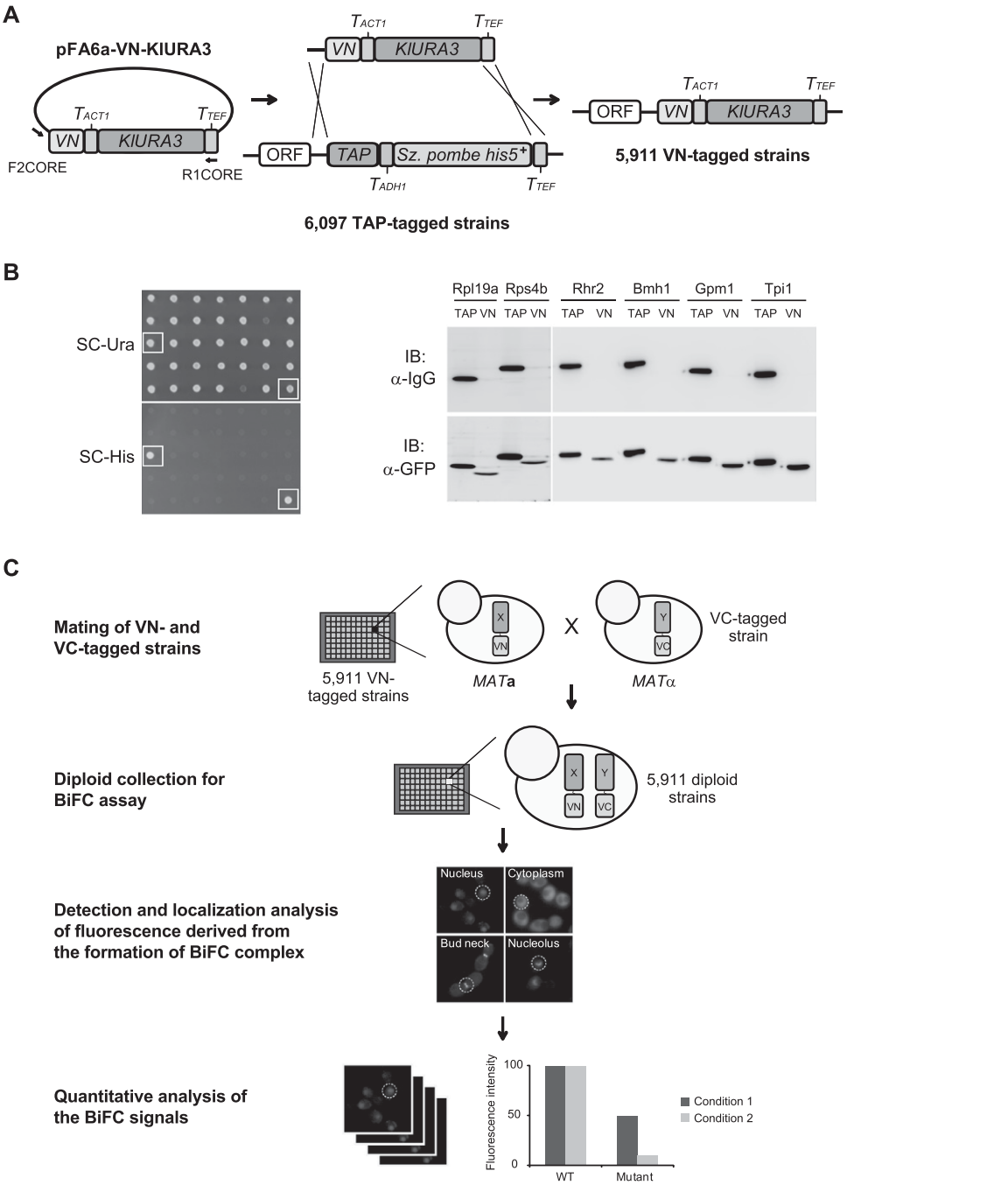

Figure 1. Construction and utilization of the VN fusion library. (*A*) Construction of the VN fusion library. A DNA fragment containing the VN tag and *KlURA3* marker sequences was amplified by PCR, using the pFA6a-VN-KlURA3 vector as the template and the primers F2CORE and R1CORE, and substituted for the C-terminal TAP tag sequence in the chromosome of each strain of the TAP fusion library by homologous recombination. KlURA3, T_{ACT1}, T_{ADH1}, and T_{TEF} represent *Kluyveromyces lactis URA3*, *S. cerevisiae ACT1* terminator, *S. cerevisiae ADH1* terminator, and *Ashbya gossypii TEF* terminator, respectively. (*B*) Confirmation of switching from the TAP tag to the VN tag. Transformed cells obtained on SC-Ura plates were replica-plated onto SC-His plates and incubated at 30°C for 3 d (*left* panel). The cells selected on SC-Ura medium and counter-selected on SC-His medium were regarded as candidates for harboring correctly switched epitopes. The cells that failed in counter-selection by SC-His are represented by open squares. Western blot analysis was performed to confirm correct switching of the VN tag from the TAP tag (*right* panel). Six highly abundant proteins (Rpl19a, Rps4b, Rhr2, Bmh1, Gpm1, and Tpi1) were selected for Western blot analysis. Both the host cells expressing the corresponding C-terminally TAP-tagged proteins (MK0074, MK0076, MK0078, MK0080, MK0082, and MK0084) and the VN-switched cells (MK0075, MK0077, MK0079, MK0081, MK0083, and MK0085) were grown to mid-log phase in YPD medium at 30°C. Total proteins were extracted, and immunoblotting was performed with HRP-conjugated anti-mouse IgG and anti-GFP antibodies. (TAP) Host strain carrying the corresponding C-terminally TAP-tagged protein. (VN) Epitope-switched strain carrying the corresponding C-terminally VN-tagged protein. (*C*) Schematic diagram of the genome-wide analysis of in vivo PPIs with the VN fusion library. For the genome-wide BiFC analysis, each strain of the VN fusion library is mated with a *MAT*α strain expressing a protein of interest tagged with the C-terminal fragment of Venus (VC), thus generating a diploid collection. Then, each strain of the diploid collection expressing both the VN fusion and the VC fusion is analyzed by fluorescence microscopy, and the images are collected and quantitatively analyzed.

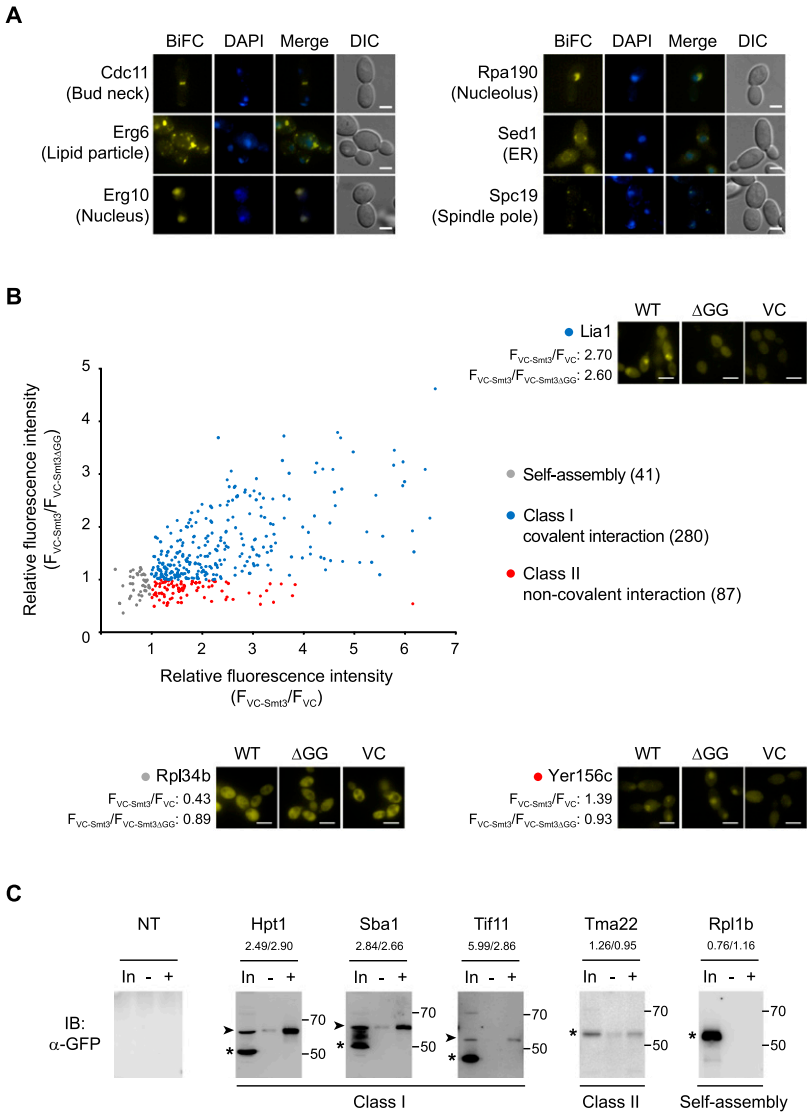

Figure 2. The SUMO interactome identified in this study. (*A*) Representative BiFC images showing in vivo SUMO interaction with diverse subcellular localizations. Fluorescence images are of the representative candidate proteins Cdc11, Erg6, Erg10, Rpa190, Sed1, and Spc19 for the bud neck, lipid particle, nucleus, nucleolus, ER, and spindle pole, respectively. Scale bars, 2 μm. (*B*) Identification and classification of the SUMO interactome. A total of 408 BiFC-positive proteins were analyzed by comparing the fluorescence intensity of cells expressing the VC fragment alone (F_{VC}) or the VC-tagged nonconjugatable Smt3 ($F_{VC\text{-}Smt3\Delta GG}$) with that of cells expressing the VC-tagged wild-type Smt3 ($F_{VC\text{-}Smt3}$). The relative BiFC intensity of $F_{VC\text{-}Smt3}/F_{VC}$ and $F_{VC\text{-}Smt3}/F_{VC\text{-}Smt3\Delta GG}$ is shown at the *x* and *y* axes, respectively. Fluorescence images are of the representative candidate proteins Rpl34b, Lia1, and Yer156c for self-assembly, class I, and class II, respectively. WT, ΔGG, and VC in the diagram indicate the representative BiFC image obtained from each analysis with the VC-tagged wild-type Smt3, the VC-tagged nonconjugatable Smt3, and the VC fragment alone, respectively. For the quantification of the BiFC signals, the mean fluorescence intensity of 20 cells for each strain was measured with custom software written in MATLAB (Mathworks). Scale bars, 5 μm. (*C*) Immunoprecipitation to validate the BiFC results. For simplicity, the results for representative proteins of the three groups (class I, class II, and self-assembly) are shown. Yeast strains expressing the GFP tag at the C terminus of the corresponding proteins (Hpt1, Sba1, Tif11, Tma22, and Rpl1b) were grown to mid-log phase in YPD medium at 30°C. Total proteins were extracted, and the fraction immunoprecipitated with or without an anti-Smt3 antibody was probed with an anti-GFP antibody. The numbers on each panel indicate the $F_{VC\text{-}Smt3}/F_{VC}$ and $F_{VC\text{-}Smt3}/F_{VC\text{-}Smt3\Delta GG}$ values for each protein. The positions of the molecular weight markers are indicated in kDas on the *right* of each panel. Arrowheads and asterisks indicate SUMO-modified and native protein bands, respectively. (NT) Nontagged cell, (In) total protein lysate, (−) immunoprecipitation without anti-Smt3 antibody, (+) immunoprecipitation with anti-Smt3 antibody.

interactome (Fig. 2B; Supplemental Fig. S3; Supplemental Table S2).

The BiFC complex formation involving SUMO can result from the covalent conjugation of SUMO to a lysine residue of a target protein or from the non-covalent interaction between SUMO and a target protein. To classify the interaction types of SUMO-interacting proteins, we constructed *MAT*α strains (HY1123 and HY1124) expressing VC fused to a wild-type Smt3 or a mutant form of Smt3 that cannot be conjugated to a target protein due to the absence of the C-terminal Gly-Gly residues (Li and Hochstrasser 1999) and mated these strains with each of the 367 VN-tagged strains identified above. We then measured the fluorescence intensity of the resulting diploid strains in which VC was fused to a wild-type Smt3 ($F_{VC\text{-}Smt3}$) or a mutant Smt3 lacking the C-terminal Gly-Gly residues ($F_{VC\text{-}Smt3\Delta GG}$). Of the 367 strains, 280 exhibited $F_{VC\text{-}Smt3}/F_{VC\text{-}Smt3\Delta GG} > 1$ (Supplemental Table S2). We classified these 280 proteins that exhibited a decrease in the BiFC signal with VC-Smt3ΔGG as class I, which is believed to be enriched for proteins that are covalently conjugated to Smt3 via the C-terminal Gly-Gly residues (Fig. 2B; Supplemental Fig. S3, blue). The remaining 87 proteins that exhibited $F_{VC\text{-}Smt3}/F_{VC\text{-}Smt3\Delta GG} \leq 1$ were classified as class II, which is believed to be enriched for proteins that interact non-covalently with Smt3 (Fig. 2B; Supplemental Fig. S3, red).

To validate the SUMO interactome identified above, we performed immunoprecipitation and assessed whether class I or II proteins exhibit appropriate covalent or non-covalent interactions with SUMO. Thirty-six class I proteins (Adk1, Aha1, Ahp1, Apt1, Arc35, Bmh1, Cdc10, Cdc33, Cpr1, Egd2, Fpr1, Gis2, Gpm1, Gre3, Hpt1, Idi1, Lia1, Mbf1, Mtq1, Pil1, Rhr2, Rnr4, Rpc40, Sba1, Sbp1, Sec21, Sec27, Ser2, Sod1, Tdh2, Tdh3, Tif11, Tsa1, Shb17, Ypl225w, and Ypr1; underlining indicates proteins identified as SUMO substrates in previous studies) and 13 class II proteins (Cbf5, Cwp2, Cys4, Dbp3, Eft1, Nop58, Pfk1, Rcl1, Rna1, Rpf2, Thr1, Tma22, and Vma4) with a broad range of $F_{VC\text{-}Smt3}/F_{VC\text{-}Smt3\Delta GG}$ values were selected and tagged with GFP. Protein extracts from cells expressing each GFP fusion protein were subject to immunoprecipitation with an anti-Smt3 antibody. The immunoprecipitated fractions were then analyzed by immunoblotting using an anti-GFP antibody to detect the pres-

ence of the original (native) or slow-migrating (SUMO-conjugated) bands of target proteins. We observed that 31 of the 36 class I proteins exhibited slow-migrating bands of SUMO-conjugated forms in the immunoprecipitated fractions, indicating that these proteins are authentic SUMO conjugation targets (Fig. 2C; Supplemental Fig. S4). For 12 class II proteins (Cbf5, Cwp2, Cys4, Dbp3, Eft1, Nop58, Pfk1, Rcl1, Rna1, Rpf2, Thr1, and Tma22), we detected only the bands of the native forms in the immunoprecipitated fractions, suggesting that these proteins interact non-covalently with SUMO. For five class I proteins (Fpr1, Gis2, Mbf1, Mtq1, and Shb17) and a class II protein (Vma4), we failed to detect protein bands in the immunoprecipitated fractions, presumably because sumoylated or SUMO-interacting forms are present at levels too low to be detected by Western blotting or are severely lost during the immunoprecipitation procedure. Another explanation would be that these proteins may have weak indirect interactions with SUMO via other SUMO-interacting proteins. As expected, Gln4, His7, Hom2, Hxk1, Lys9, Rpl1b, and Zuo1, which showed false-positive BiFC signals in the self-assembly test, exhibited no interaction with SUMO. These results suggest that our approach of using $F_{VC\text{-}Smt3}/F_{VC}$ and $F_{VC\text{-}Smt3}/F_{VC\text{-}Smt3\Delta GG}$ values is reliable not only for identifying the SUMO interactome but also for classifying the interaction types of the SUMO interactome.

Characterization of the SUMO interactome

Previous systematic PPI analyses have identified 781 SUMO target proteins (Panse et al. 2004; Wohlschlegel et al. 2004; Zhou et al. 2004; Denison et al. 2005; Hannich et al. 2005; Wykoff and O'Shea 2005; Makhnevych et al. 2009). In this study, we identified 367 SUMO target proteins; 143 of these overlapped with the 781 proteins in previous data sets, but another 224 were newly defined (Fig. 3A). Our data set showed a modest concordance with previous reports from Zhou et al. (2004) (41%), Panse et al. (2004) (29%), and Hannich et al. (2005) (27%) (Fig. 3B). Previous large-scale studies to identify SUMO target proteins have primarily been performed with the yeast two-hybrid method and TAP-MS, which do not measure PPI in the natural cellular context. The identification of 224 new SUMO targets in this study reflects the difference in the employed experimental methods between this study and previous studies and, thus, our data set appears to be highly complementary to the existing data sets.

We also believe that the rather low overlap between previous data sets and our data set is partly due to the topological constraints in the BiFC complex formation (Hu et al. 2002; Hu and Kerppola 2003; Sung and Huh 2007). It is estimated that BiFC can occur when VN and VC are fused to positions that are separated by a distance no greater than ~10 nm, provided that there is sufficient flexibility to permit the association of the fragments (Hu et al. 2002). In our VN fusion library, each endogenous gene is tagged with VN at its C-terminal end to ensure that each fusion protein can be expressed from its own native promoter. Thus, if the site for SUMO interaction in a given SUMO target protein is located away from its C terminus, the BiFC signal is not likely to be detected for the protein. To test this notion, we tagged VN at the N terminus of 10 proteins (Aos1, Cdc3, Hsp82, Htb1, Pol30, Rap1, Rsc58, Top1, Tfg1, and Ubc9) that have been identified as SUMO targets in previous studies but not in this study. When these N-terminally VN-tagged proteins were analyzed for BiFC with VC-Smt3, eight of the 10 proteins (except Htb1 and Tfg1) exhibited positive BiFC signals (Supplemental Fig. S5). This observation suggests that several proteins tagged with VN at their C termini are subject to topological constraints in the BiFC complex formation and are thus included in the false-negative group in our data set.

A gene ontology (GO) analysis revealed that the SUMO target proteins identified in this study can be categorized into a variety of biological processes (Supplemental Table S3). In addition to the expected roles of SUMO in transcription, nucleic acid metabolism, and transport, the GO analysis suggests several interesting roles of SUMO in a wide range of processes including ribosome biogenesis, translation, and stress response. Notably, class I proteins that are believed to be covalently conjugated to Smt3 were overrepresented in the biological processes of cell-cycle checkpoint, regulation of cell cycle, post-transcriptional regulation of gene expression, response to oxidative stress, nuclear transport, de novo protein folding, and regulation of proteolysis, while class II proteins that are believed to be interacting non-covalently with Smt3 were overrepresented in the biological processes of DNA packaging, chromatin organization, chromatin assembly or disassembly, and RNA processing.

Previous reports have demonstrated the nuclear localization of proteins involved in the SUMO conjugation pathway, such as Aos1, Ubc9, and Smt3, and SUMO-specific proteases Ulp1 and Ulp2 (Li and Hochstrasser 2000; Huh et al. 2003), suggesting that sumoylation may play critical roles in the nuclear processes. Consistent with this expectation, ~43% of SUMO target proteins identified in this study were located in the nuclear regions (nucleus and nucleolus), according to the yeast GFP fusion localization database (Fig. 3C; Huh et al. 2003). Notably, SUMO target proteins were significantly enriched in the nucleolus ($P = 2.15 \times 10^{-15}$) and the spindle pole ($P = 1.60 \times 10^{-2}$), which have not previously been highlighted as sites for sumoylated or SUMO-interacting proteins.

One of the advantages of the BiFC assay is that it can directly provide information about the subcellular localization of PPIs. In this study, the subcellular region in which the BiFC signal for a protein is detected represents the localization of the protein directly modified by or non-covalently interacting with SUMO. The distribution of the subcellular localization of BiFC signals revealed that ~89% of the 367 BiFC signals were detected in the nuclear and cytoplasmic region (nucleus, nucleolus, and cytoplasm), while the BiFC signals for 41 proteins were found in other subcellular regions, such as the spindle pole, the ER, the bud neck, and the mitochondrion (Fig. 3D). A comparison of subcellular localization between the BiFC signals for the SUMO interactome and the GFP signals for the corresponding proteins revealed that the BiFC and GFP signals yielded identical localization patterns for ~64% of the proteins (Fig. 3E). However, for 105 proteins, the BiFC signal for the SUMO interaction was partially localized within a region in which the corresponding GFP fusion protein was detected. More surprisingly, the subcellular localization of the BiFC signals for 26 proteins was different from that of the corresponding GFP fusions. This result is not only consistent with the notion that only a small fraction of target proteins are sumoylated (Geiss-Friedlander and Melchior 2007) but also suggests that the subcellular localization of the sumoylated forms of some target proteins is differentially regulated from that of the nonsumoylated forms.

Differences in substrate specificity between Ulp1 and Ulp2

Elegant studies describing the detailed molecular features of the SUMO-specific proteases Ulp1 and Ulp2 in *S. cerevisiae* expanded the understanding of regulatory circuits in the SUMO pathway (Li and Hochstrasser 1999, 2000). The SUMO conjugation pattern is distinct for each mutant of *ULP1* and *ULP2*, suggesting that Ulp1

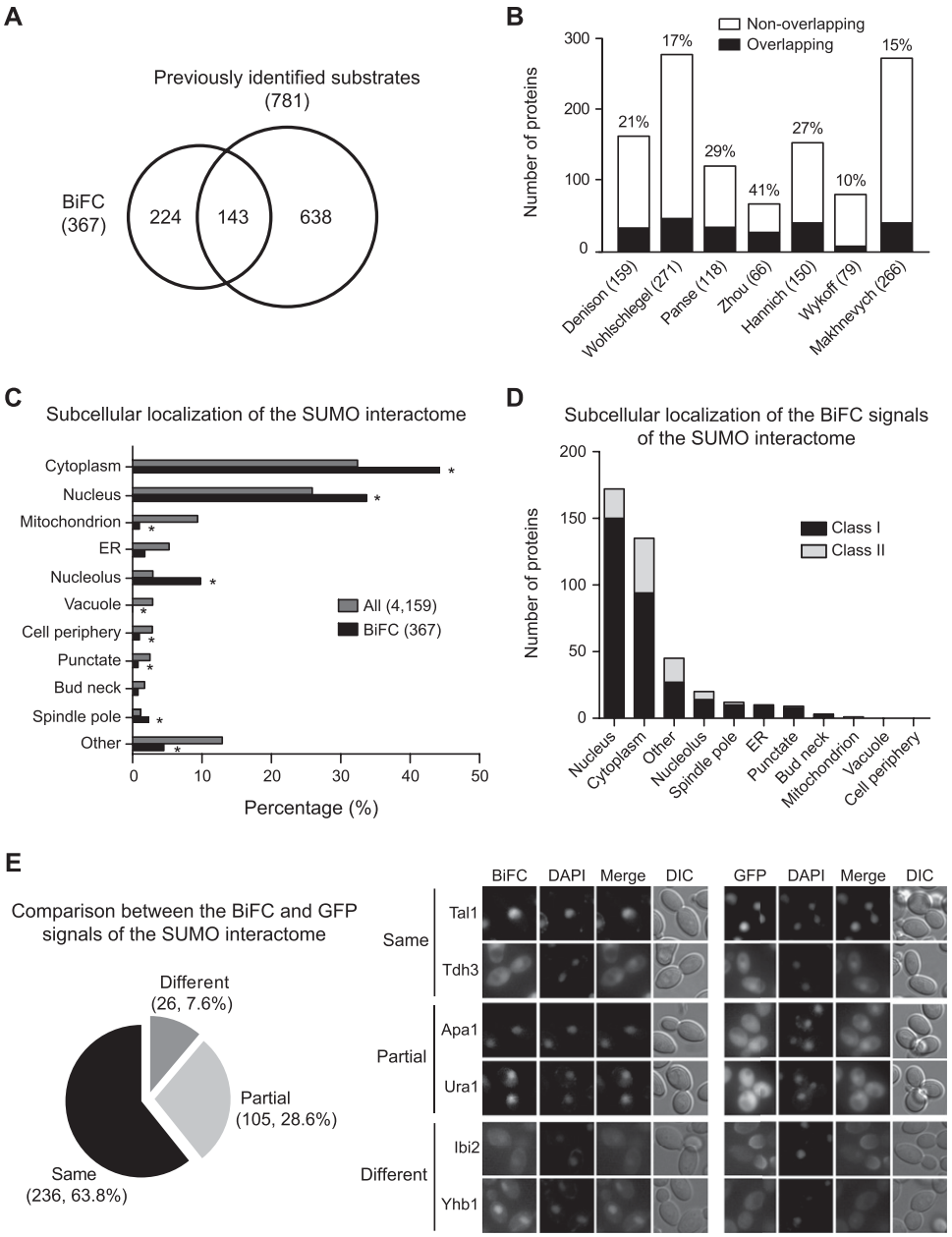

Figure 3. Characterization of the SUMO interactome. (*A*) Venn diagram depicting the comparison of the SUMO substrates identified in this study and those identified in seven previous analyses. (*B*) Bar graph depicting the comparison between the SUMO interactome and each of the seven previous data sets. The black and white bars indicate the number of SUMO substrates that overlap and do not overlap, respectively, with the data set in this study. The percentage of concordance between data sets is indicated *above* the bars. Numbers in parentheses indicate the number of SUMO substrates identified in each study. (*C*) Percentage of total hits for each subcellular localization of the SUMO substrates from the two data sets (All and BiFC). (All) Whole proteins for which subcellular localization has been annotated in the yeast GFP fusion localization database (http://yeastgfp.yeastgenome.org). (BiFC) SUMO interactome identified in this study. (Asterisks) Significant difference compared with All ($P < 0.05$; two-sided Fisher's exact test). (*D*) The number of hits for each subcellular localization of the BiFC signals. The black and gray bars indicate the number of substrates belonging to class I and class II, respectively. (*E*) (*Left* panel) Venn diagram depicting the comparison between the BiFC signal and GFP signal of each protein in the SUMO interactome. (*Right* panel) Fluorescence images of Tal1 and Tdh3, Apa1 and Ura1, and Ibi2 and Yhb1, which exhibit the same, partial, and different localization, respectively, between the BiFC and GFP signals.

and Ulp2 desumoylate different sets of target proteins. However, the specific differences in substrate specificity and biological function between Ulp1 and Ulp2 remain unclear due to a lack of appropriate experimental methods. Previously, we have demonstrated the feasibility of quantitatively analyzing protein desumoylation by Ulp1 using the BiFC assay (Sung and Huh 2010). To apply the same approach to identify the substrates of SUMO-specific proteases, we first generated *MAT*α strains (HY1130 and HY1131) expressing either Ulp1 or Ulp2 from the inducible *GAL1* promoter on a CEN plasmid and VC-tagged Smt3. HY1130 and HY1131 cells expressing Ulp1 and Ulp2, respectively, from the inducible *GAL1* promoter exhibited severe growth defects on galactose-containing

medium compared with control HY1129 cells carrying an empty plasmid (data not shown), indicating that the abnormally excessive desumoylation resulting from overexpression of Ulp1 and Ulp2 is harmful to cells. HY1130 and HY1131 strains were mated with each of the 280 VN-tagged strains expressing class I proteins, and the normalized BiFC signal intensity of cells overexpressing Ulp1 ($F_{Ulp1} = F_{Ulp1\_raffinose}/F_{Ulp1\_galactose}$) or Ulp2 ($F_{Ulp2} = F_{Ulp2\_raffinose}/F_{Ulp2\_galactose}$) was compared with that of control cells without overexpression of Ulps ($F_{control} = F_{control\_raffinose}/F_{control\_galactose}$). Several strains exhibited Ulp1- or Ulp2-specific changes in the BiFC signal intensity. Based on the change in the BiFC signal intensity, we classified 280 proteins into four groups as follows: (1) 80 putative candidates for Ulp1-specific substrates ($F_{Ulp1}/F_{control} > 1$, $F_{Ulp2}/F_{control} \leq 1$); (2) 47 putative candidates for Ulp2-specific substrates ($F_{Ulp1}/F_{control} \leq 1$, $F_{Ulp2}/F_{control} > 1$); (3) 44 putative candidates for both Ulp1- and Ulp2-specific substrates ($F_{Ulp1}/F_{control} > 1$, $F_{Ulp2}/F_{control} > 1$); and (4) the remaining 109 proteins ($F_{Ulp1}/F_{control} \leq 1$, $F_{Ulp2}/F_{control} \leq 1$), which were not included in any of the above groups (Fig. 4A; Supplemental Table S4). It is not yet clear whether the remaining 109 proteins are Ulp1- or Ulp2-specific substrates.

To validate the Ulps substrate classification based on quantitative BiFC assay, cells expressing the GFP-tagged candidate proteins were analyzed by Western blotting. Ser2 was classified into the group of the putative candidates for both Ulp1- and Ulp2-specific substrates. Consistent with the results of the BiFC assay, the slow-migrating band corresponding to the SUMO-conjugated Ser2 significantly decreased under overexpression of either Ulp1 or Ulp2 (Fig. 4B). Bmh1, a putative candidate for a Ulp1-specific substrate, exhibited a considerable decrease in its SUMO-conjugated band under overexpression of Ulp1 but not Ulp2. In the case of Ald6, which was classified into the group of putative candidates for Ulp2-specific substrates, we could not detect its SUMO-conjugated band in Western blotting. Interestingly, the native band of Ald6 considerably decreased under overexpression of Ulp2. Although it is not clear at present whether Ulp2 directly desumoylates Ald6, it seems that Ald6 is subject to SUMO-dependent stabilization and that Ulp2 plays a specific role in the regulation of Ald6 stability. Overall, these results suggest that our quantitative BiFC assay with overexpressed Ulps can be used for preliminary identification of Ulp1- and Ulp2-specific substrates.

Because SUMO can control the biological functions of target proteins by modulating their activity, localization, or stability, we assumed that desumoylation by Ulps overexpression may induce changes in the activity, localization, or amount of target proteins. To evaluate this possibility, we examined the localization and amount of GFP fusions of 171 proteins that exhibited Ulp1- or Ulp2-specific decreases in the BiFC signal intensity. Of 171 proteins, 27 and 10 exhibited significant changes in their subcellular localization and amount, respectively, under overexpression of Ulps (Fig. 4C; Supplemental Table S5). Of these 37 proteins, the changes in the subcellular localization or amount of 26 were specifically dependent on Ulp1, while the changes of three of them were specifically dependent on Ulp2. These observations demonstrate that SUMO and Ulps are directly or indirectly involved in the regulation of the localization and amount of several SUMO substrates and support the notion that Ulp1 and Ulp2 target different sets of proteins.

Cell cycle and SUMO

SUMO seems to play important roles in cell cycle regulation. Many proteins involved in cell-cycle progression and regulation in *S. cerevisiae* are SUMO substrates (Panse et al. 2004; Wohlschlegel

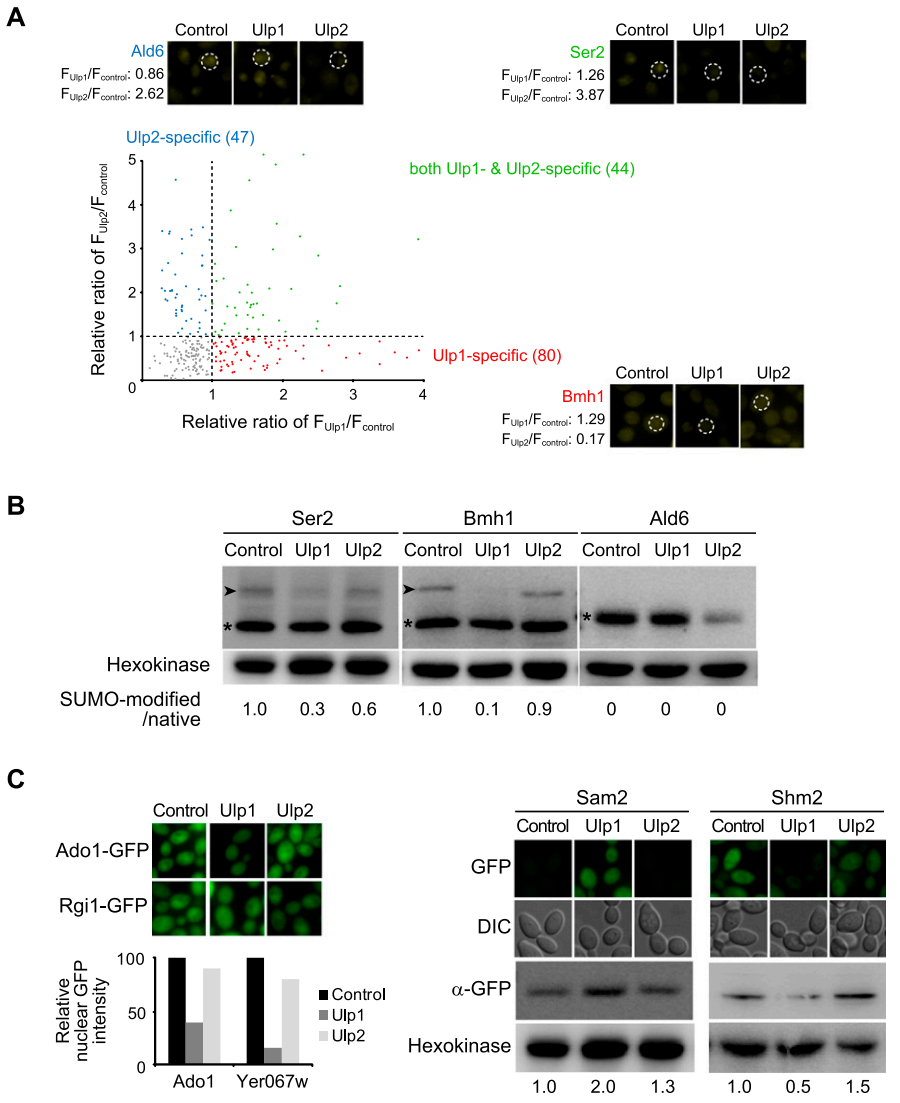

Figure 4. (Legend on next page)

et al. 2004; Zhou et al. 2004; Denison et al. 2005; Hannich et al. 2005; Wykoff and O'Shea 2005; Makhnevych et al. 2009). In addition, *ubc9* mutants, which exhibit defects in the SUMO conjugation pathway, exhibit a G2/M cell cycle arrest (Seufert et al. 1995). Our observation that the SUMO interactome is highly enriched in biological processes related to the cell cycle (Fig. 5A; Supplemental Fig. S3; Supplemental Table S3) also supports a role for SUMO in the regulation of the biological functions of target proteins during the cell cycle. We further investigated whether the SUMO interaction pattern of cell-cycle-related proteins is changed at specific cell-cycle stages. To do this, we analyzed the changes in the BiFC signal of 34 cell-cycle-related proteins identified as class I or II substrates (Ask1, Bfr1, Bmh1, Bmh2, Bur2, Cdc10, Cdc11, Cdc14, Cdc28, Cdc33, Cka2, Ckb1, Cks1, Cpr1, Dad3, Duo1, Fpr3, Glc7, Mtw1, Net1, Nnf1, Nsl1, Rad9, Rfc3, Rsc6, Shs1, Slk19, Spc19, Spc24, Spc34, Stu2, Tid3, Tpd3, and Wtm1) in the presence of hydroxyurea or nocodazole, which induce cell-cycle arrest at S and M phase, respectively. Among the 34 proteins, 12 (Bmh1, Bmh2, Bur2, Cdc28, Cdc33, Ckb1, Cks1, Glc7, Rfc3, Spc19, Tpd3, and Wtm1) exhibited noticeable changes in the BiFC signal intensity in the presence of hydroxyurea or nocodazole (Fig. 5B). For example, Glc7 exhibited a considerable increase in the BiFC signal under nocodazole treatment, while Cdc28, Tpd3, and Wtm1 exhibited a brighter BiFC signal under hydroxyurea treatment than the control (Fig. 5C). The levels of 12 proteins and Smt3 were not significantly changed in hydroxyurea- or nocodazole-treated cells (Supplemental Fig. S6), indicating that the changes in the BiFC signal for these proteins are caused by an alteration in their interaction with SUMO rather than an alteration in their abundance. Taken together, our observations suggest that the interaction of these proteins with SUMO is regulated in a cell-cycle-dependent manner and that SUMO may modulate the biological functions of these proteins during the cell cycle.

Discussion

In the present study, we generated a collection of yeast strains expressing full-length proteins tagged with VN from their own native promoters and performed a genome-wide SUMO interactome screen with the BiFC assay. Using this approach, we systematically identified the SUMO interactome, which comprises 367 proteins, and confirmed that several of these proteins are authentic SUMO targets by immunoprecipitation and Western blotting. Because of the advantages of the BiFC assay, we could obtain previously unavailable information about the SUMO interactome, including the subcellular localization of protein sumoylation, the type of interaction between SUMO and target proteins, and the substrate specificity of the SUMO-specific proteases Ulp1 and Ulp2. For example, we found that SUMO target proteins are significantly enriched in the nucleolus and the spindle pole, which have not previously been highlighted as sites for sumoylated or SUMO-interacting proteins. It will be interesting to investigate whether and how SUMO regulates the functions of the spindle pole body and the nucleolus by modulating the activity of its target proteins in these organelles. In addition, by examining the localization and amount of GFP fusions of 171 proteins that exhibited Ulp1- or Ulp2-specific decreases in the BiFC signal intensity, we could identify 37 proteins exhibiting significant changes in their subcellular localization or amount under overexpression of Ulps. It will be worthwhile to investigate whether the changes in the localization or amount of these proteins induced by overexpression of Ulps affect their biological functions. We also found that several proteins exhibit cell-cycle-dependent changes in the interaction with SUMO. Whether and how SUMO regulates the biological functions of these proteins during the cell cycle remain to be further studied. Notably, our data set includes 224 SUMO target proteins that have been missed in previous studies due to various technical limitations. These newly identified SUMO targets may be promising candidates for further investigations that will provide significant insights into the functional roles of SUMO in a number of biological processes.

Although the BiFC assay is a very powerful method for detecting in vivo PPIs as demonstrated in this study, there are several potential caveats to be considered. First, the BiFC complex can be irreversibly formed, as seen in vitro and under some in vivo conditions (Hu et al. 2002; Kerppola 2008), and thus it may affect the dynamics of complex dissociation and partner exchange. However, several recent studies have shown that the BiFC complex formation can occur in a reversible manner (Schmidt et al. 2003; Blondel et al. 2005; Guo et al. 2005; Cole et al. 2007; Sung and Huh 2007). It is likely that the reversibility of BiFC complex formation is dependent on the cel-

Figure 4. Substrate specificities of SUMO-specific proteases. (*A*) Classification of the substrate specificities of SUMO-specific proteases. A total of 280 class I proteins were analyzed by comparing the normalized BiFC intensity of cells overexpressing Ulp1 ($F_{Ulp1} = F_{Ulp1\_raffinose}/F_{Ulp1\_galactose}$) or Ulp2 ($F_{Ulp2} = F_{Ulp2\_raffinose}/F_{Ulp2\_galactose}$) with that of cells without overexpressing Ulps ($F_{control} = F_{control\_raffinose}/F_{control\_galactose}$). The relative ratios of $F_{Ulp1}/F_{control}$ and $F_{Ulp2}/F_{control}$ for the 280 proteins are represented on the plot. Representative BiFC images of Ser2, Bmh1, and Ald6 for both Ulp1- and Ulp2-specific, Ulp1-specific, and Ulp2-specific substrates, respectively, are also shown. Control, Ulp1, and Ulp2 in the diagram indicate cells containing p415GAL, p415GAL-Ulp1, and p415GAL-Ulp2, respectively. For overexpression of Ulps, cells were grown in synthetic medium containing raffinose until mid-log phase and then transferred to and incubated in synthetic medium containing galactose for 2 h at 30°C. For the quantification of the BiFC signals, the mean fluorescence intensity of 20 cells for each strain was measured with custom software written in MATLAB (Mathworks). (*B*) Western blot analysis to validate Ulp1- and Ulp2-specific substrates. Immunoblots of Ser2, Bmh1, and Ald6 for both Ulp1- and Ulp2-specific, Ulp1-specific, and Ulp2-specific substrates, respectively, are shown. Yeast strains expressing the corresponding GFP fusion proteins with p415GAL, p415GAL-Ulp1, or p415GAL-Ulp2 were grown as described above. Total proteins were extracted, and immunoblotting was performed with a HRP-conjugated anti-GFP antibody. Hexokinase was detected with an anti-hexokinase antibody as an internal control. The relative ratio of SUMO-modified protein to native protein, normalized against that of the control without Ulps expression, is shown below each lane. Control, Ulp1, and Ulp2 in the diagram indicate extracts from cells containing p415GAL, p415GAL-Ulp1, and p415GAL-Ulp2, respectively. Arrowheads and asterisks indicate SUMO-modified and native protein bands, respectively. (*C*) Microscopic and Western blotting results showing the changes in the localization and the amount of proteins under overexpression of Ulps. (*Left* panel) Representative fluorescence images showing the changes in the localization of proteins under overexpression of Ulps. Yeast strains expressing the corresponding GFP fusion proteins with p415GAL, p415GAL-Ulp1, or p415GAL-Ulp2 were grown as described above. Control, Ulp1 and Ulp2 in the diagram indicate cells containing p415GAL, p415GAL-Ulp1, and p415GAL-Ulp2, respectively. For the quantification of the nuclear GFP signals, the mean fluorescence intensity of 20 cells for each strain was measured with custom software written in MATLAB (Mathworks). (*Right* panel) Representative Western blotting results showing the changes in the amount of proteins under overexpression of Ulps. Yeast strains expressing the corresponding GFP fusion proteins with p415GAL, p415GAL-Ulp1, or p415GAL-Ulp2 were grown as described above. Total proteins were extracted, and immunoblotting was performed with a HRP-conjugated anti-GFP antibody. Hexokinase was detected with an anti-hexokinase antibody as an internal control. The relative protein level is shown *below* each lane.

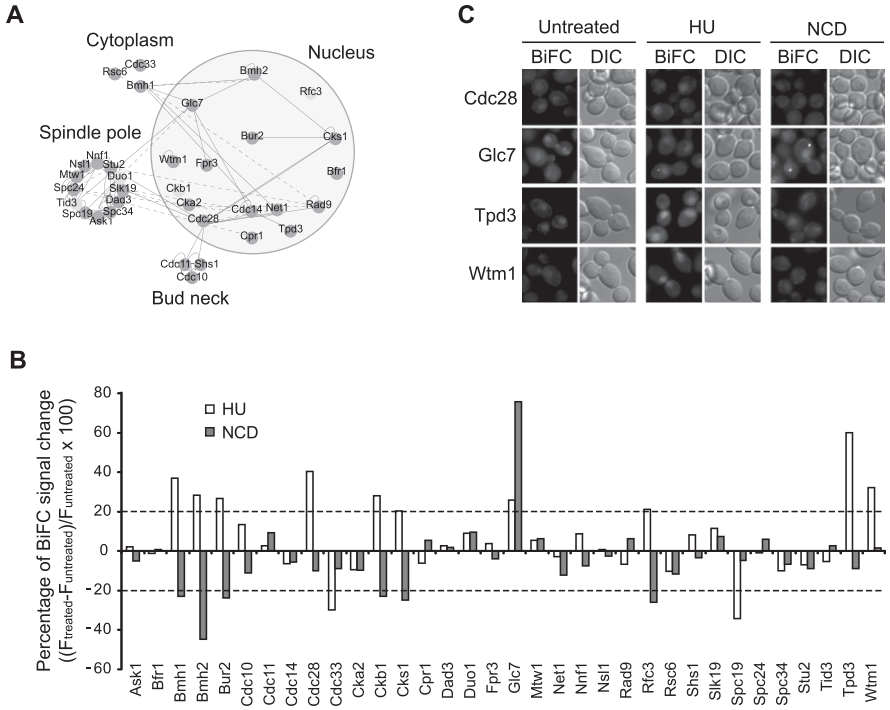

Figure 5. Cell cycle and the SUMO pathway. (*A*) A SUMO subnetwork highlighting the relationship between cell-cycle progression and the SUMO pathway. The dark gray and light gray circles represent class I and class II substrates, respectively. The solid and dashed lines indicate physical and genetic interactions between two proteins, respectively. (*B*) Quantitative analysis of SUMO interaction of 34 cell-cycle-related proteins in the presence of hydroxyurea or nocodazole. Cells coexpressing the corresponding VN-tagged proteins and VC-tagged Smt3 were grown to mid-log phase in synthetic medium, aliquoted, and treated with 0.2 M hydroxyurea or 15 μg/mL nocodazole. After incubation for 3 h, the percentage of the change in BiFC signal intensity of cells was analyzed. For the quantification of the BiFC signals, the mean fluorescence intensity of 20 cells for each strain was measured with custom software written in MATLAB (Mathworks). HU and NCD indicate the treatments with hydroxyurea and nocodazole, respectively. (Dashed lines) A cut-off value of ±20%. (*C*) Fluorescence images of cells coexpressing the corresponding VN-tagged proteins and VC-tagged Smt3 in the presence of hydroxyurea or nocodazole. Cells were grown and treated with the inhibitors as described above.

lular context or the stability of the complex. The reversibility of BiFC complex formation also seems to be related to the expression level of the fluorescent protein fragments fused to the interacting proteins, given that all reported cases of irreversible BiFC complex formation employed highly expressed fluorescent protein fragments under the control of strong constitutive promoters. In this regard, our VN fusion library, in which the VN tag is expressed from the native promoter of each fused protein, will be useful for the genome-wide BiFC assay with minimized irreversible BiFC complex formation. Second, the BiFC complex formation is subject to topological constraints. It is estimated that BiFC can occur when VN and VC are fused to positions that are separated by a distance no greater than ~10 nm (Hu et al. 2002). Because each endogenous gene is tagged with VN at its C-terminal end in our VN fusion library, if the site for SUMO interaction in a given SUMO target protein is located away from its C terminus, the BiFC signal is not likely to be detected for the protein. By tagging VN at the N terminus of 10 proteins that have been identified as SUMO targets in previous studies but not in this study, we could demonstrate the presence of topological constraints in the BiFC complex formation (Supplemental Fig. S5). The future construction of an N-terminally VN-tagged strain collection and its utilization, together with the C-terminally VN-tagged collection, will help alleviate the topological problems in genome-wide BiFC screens and greatly reduce false-negative results. Third, the BiFC assay alone is not sufficient to determine whether the putative SUMO substrates are directly covalently modified by SUMO or are associated non-covalently with a SUMO substrate in close enough proximity to facilitate the BiFC complex formation. Two hundred eighty class I proteins, which exhibited a decrease in the BiFC signal with VC-Smt3ΔGG (Fig. 2B), are believed to be enriched for proteins that are covalently conjugated to SUMO via the C-terminal Gly-Gly residues. However, some class I proteins may interact non-covalently with other endogenous proteins that are actually covalently attached to SUMO. Further analyses (e.g., Western blotting and mass spectrometry) will be required to confirm whether each of the class I proteins is directly covalently modified by SUMO. Fourth, the BiFC assay does not enable real-time detection of complex formation due to slow fluorophore maturation of the BiFC complex (Hu et al. 2002; Sung and Huh 2010). Therefore, the localization of the BiFC signal does not always represent the subcellular regions where the two proteins initially interact with each other; the BiFC signal may develop later in a different location after their initial interaction has occurred, particularly for a dynamic protein complex. This case may be relevant to some of the proteins for which the subcellular localization of the BiFC signals was partially localized within or different from that of the corresponding GFP fusions (Fig. 3E).

In the last decade, yeast epitope (e.g., GFP, TAP, and GST) fusion collections have opened new horizons for functional proteomic research. The yeast VN fusion collection constructed in this study, which covers 95% of all ORFs, will be another valuable resource for functional proteomic studies by facilitating in vivo genome-wide analysis of binary PPIs using the BiFC method. As shown in this study, a genome-wide screen with the VN fusion library provides comprehensive information on the occurrence, localization, and extent of PPIs that is not obtainable by conventional approaches. Furthermore, because of the particular advantage of the BiFC assay in the quantitative measurement of PPIs in living cells, the VN fusion library is a powerful tool for analyzing not only PPIs under normal steady-state conditions but also the global alteration of PPIs in response to specific external stimuli or growth conditions. Future investigations into these dynamic PPI networks will provide a new dimension of information valuable for functional annotations of unknown proteins and will reveal fundamental mechanisms of cellular regulatory processes.

Methods

Yeast strains and culture conditions

S. cerevisiae strains used in this study are listed in Supplemental Table S6. Yeast cells were grown at 30°C in YPD (1% yeast extract,

2% peptone, and 2% glucose) or synthetic complete (SC) medium lacking appropriate amino acids for selection (Sherman 2002). For solid media, 2% agar was added. For the ectopic overexpression of a protein of interest from an inducible *GAL1* promoter, cells were grown to mid-log phase in medium containing raffinose and then transferred to and incubated in medium containing galactose.

Construction of plasmids

For the construction of the pFA6a-VN-KlURA3 vector, ~500 bp of the PacI-AscI-digested VN tag was obtained from pFA6a-VN-His3MX6 and ligated into the PacI-AscI-digested pFA6a-GFP-KlURA3 vector described in a previous report (Sung et al. 2008). To classify interaction type between SUMO and target proteins using the BiFC assay, we expressed the wild-type and mutant type of Smt3 lacking Gly-Gly residues from the *TEF* promoter on pRS413 expression vectors. To do this, the ~600-bp PCR product of the VC-SMT3 region was obtained using HY1121 genomic DNA as a template, forward primer P1, and reverse primers P2 and P3 for the wild-type and mutant type of Smt3, respectively. The PCR product was digested with XbaI and XhoI and ligated into the XbaI-XhoI-digested p413TEF plasmid. In addition, we constructed an expression vector containing only the VC fragment with the same *TEF* promoter for the self-assembly test. The ~300-bp PCR product of the VC region, obtained using HY1121 genomic DNA as a template, forward primer P4, and reverse primer P5, was digested with EcoRI and XhoI and ligated into the EcoRI-XhoI-digested p413TEF plasmid, thus generating the p413TEF-VC vector. Construction of the p415GAL-Ulp1 vector for ectopic expression of SUMO-specific protease Ulp1 is described in a previous report (Sung and Huh 2010). For ectopic expression of SUMO-specific protease Ulp2, the ~1800-bp PCR product of *ULP2* was obtained using BY4741 genomic DNA as a template, forward primer P11, and reverse primer P12. The PCR product was digested with XbaI and XhoI, and ligated into the XbaI-XhoI-digested p415GAL plasmid, thus generating p415GAL-Ulp2.

Construction of the VN-tagged strain collection

A chromosomally VN-tagged strain collection was generated from the TAP-tagged collection (Ghaemmaghami et al. 2003), using the epitope switching strategy described previously (Sung et al. 2008). An epitope switching module containing the VN tag and *KlURA3* marker sequences was amplified by PCR with pFA6a-VN-KlURA3 as the template and a universal primer set F2CORE and R1CORE (Supplemental Table S1). The resulting module was transformed into each strain of the TAP-tagged strain collection, which consists of 6097 *MAT***a** strains with chromosomal C-terminally TAP-tagged ORFs. Transformed cells were spread on SC-Ura plates and incubated at 30°C for 3 d. To confirm correct switching from the TAP tag to the VN tag, colonies selected on SC-Ura medium were counter-selected on SC-His medium.

Quantitative analysis of fluorescent images

Fluorescence microscopy was performed as previously described (Sung and Huh 2007). Quantification of fluorescent images (BiFC and GFP) was performed as previously described with some modifications (Benanti et al. 2007). MATLAB identified the nuclear region stained with DAPI as objects. In the FITC channel, fluorescence was quantified in an area larger than the original mask. Because the bud neck was excluded from the region that was quantified, fluorescent signals localizing to the bud neck were examined manually.

Western blot analysis

Cell extracts were prepared as previously described (Sung et al. 2008). SDS-PAGE and Western blot analysis were performed using standard methods with a HRP-conjugated anti-mouse IgG antibody (A9044, Sigma), a HRP-conjugated anti-GFP antibody (600-103-215, Rockland), an anti-Smt3 antibody (200-401-428, Rockland), and an anti-hexokinase antibody (H2035-02, United States Biological).

Immunoprecipitation assay

Cell extracts were prepared as previously described (Sung et al. 2008). An anti-Smt3 antibody (200-401-428, Rockland) was added to cell extracts and incubated with gentle rocking overnight at 4°C. Protein A-agarose (P3476, Sigma) was added to the immunoprecipitation reaction and incubated with gentle rocking for 2 h at 4°C. Beads were washed three times with 25 mM Tris, pH 7.5, 150 mM NaCl, and 0.2% NP40. After the final wash with the same buffer without detergent, beads were resuspended in 2× SDS buffer and loaded on SDS-PAGE gels. Proteins were detected with a HRP-conjugated anti-GFP antibody (600-103-215, Rockland).

Acknowledgments

We thank Hee Seung Choi for assistance in MATLAB programming, Dr. Daehyun Baek for assistance in bioinformatic analysis, and Dr. Chang-Deng Hu for generously providing plasmids containing VN and VC sequences. We also thank members of the Huh laboratory for helpful discussions. This work was supported by the 21C Frontier Microbial Genomics and Application Center Program (MG-11-2008-09-004-00), the 21C Frontier Functional Proteomics Project (FPR08A1-060), the SRC/ERC Program (2011-0006426), and the Basic Science Research Program (2010-0022887) through the National Research Foundation of Korea funded by the Ministry of Education, Science and Technology, Republic of Korea.

References

Benanti JA, Cheung SK, Brady MC, Toczyski DP. 2007. A proteomic screen reveals SCF^{Grr1} targets that regulate the glycolytic-gluconeogenic switch. *Nat Cell Biol* **9:** 1184–1191.

Blondel M, Bach S, Bamps S, Dobbelaere J, Wiget P, Longaretti C, Barral Y, Meijer L, Peter M. 2005. Degradation of Hof1 by SCF^{Grr1} is important for actomyosin contraction during cytokinesis in yeast. *EMBO J* **24:** 1440–1452.

Cole KC, McLaughlin HW, Johnson DI. 2007. Use of bimolecular fluorescence complementation to study in vivo interactions between Cdc42p and Rdi1p of *Saccharomyces cerevisiae*. *Eukaryot Cell* **6:** 378–387.

Denison C, Rudner AD, Gerber SA, Bakalarski CE, Moazed D, Gygi SP. 2005. A proteomic strategy for gaining insights into protein sumoylation in yeast. *Mol Cell Proteomics* **4:** 246–254.

Fang DY, Kerppola TK. 2004. Ubiquitin-mediated fluorescence complementation reveals that Jun ubiquitinated by Itch/AIP4 is localized to lysosomes. *Proc Natl Acad Sci* **101:** 14782–14787.

Fields S, Song O. 1989. A novel genetic system to detect protein-protein interactions. *Nature* **340:** 245–246.

Gavin AC, Bosche M, Krause R, Grandi P, Marzioch M, Bauer A, Schultz J, Rick JM, Michon AM, Cruciat CM, et al. 2002. Functional organization of the yeast proteome by systematic analysis of protein complexes. *Nature* **415:** 141–147.

Gavin AC, Aloy P, Grandi P, Krause R, Boesche M, Marzioch M, Rau C, Jensen LJ, Bastuck S, Dumpelfeld B, et al. 2006. Proteome survey reveals modularity of the yeast cell machinery. *Nature* **440:** 631–636.

Geiss-Friedlander R, Melchior F. 2007. Concepts in sumoylation: A decade on. *Nat Rev Mol Cell Biol* **8:** 947–956.

Ghaemmaghami S, Huh W, Bower K, Howson RW, Belle A, Dephoure N, O'Shea EK, Weissman JS. 2003. Global analysis of protein expression in yeast. *Nature* **425:** 737–741.

Ghosh I, Hamilton AD, Regan L. 2000. Antiparallel leucine zipper-directed protein reassembly: Application to the green fluorescent protein. *J Am Chem Soc* **122:** 5658–5659.

Guo Y, Rebecchi M, Scarlata S. 2005. Phospholipase Cβ2 binds to and inhibits phospholipase Cδ1. *J Biol Chem* **280:** 1438–1447.
Hannich JT, Lewis A, Kroetz MB, Li SJ, Heide H, Emili A, Hochstrasser M. 2005. Defining the SUMO-modified proteome by multiple approaches in *Saccharomyces cerevisiae*. *J Biol Chem* **280:** 4102–4110.
Ho Y, Gruhler A, Heilbut A, Bader GD, Moore L, Adams SL, Millar A, Taylor P, Bennett K, Boutilier K, et al. 2002. Systematic identification of protein complexes in *Saccharomyces cerevisiae* by mass spectrometry. *Nature* **415:** 180–183.
Hu CD, Kerppola TK. 2003. Simultaneous visualization of multiple protein interactions in living cells using multicolor fluorescence complementation analysis. *Nat Biotechnol* **21:** 539–545.
Hu CD, Chinenov Y, Kerppola TK. 2002. Visualization of interactions among bZIP and Rel family proteins in living cells using bimolecular fluorescence complementation. *Mol Cell* **9:** 789–798.
Huh WK, Falvo JV, Gerke LC, Carroll AS, Howson RW, Weissman JS, O'Shea EK. 2003. Global analysis of protein localization in budding yeast. *Nature* **425:** 686–691.
Ito T, Chiba T, Ozawa R, Yoshida M, Hattori M, Sakaki Y. 2001. A comprehensive two-hybrid analysis to explore the yeast protein interactome. *Proc Natl Acad Sci* **98:** 4569–4574.
Johnsson N, Varshavsky A. 1994. Split ubiquitin as a sensor of protein interactions in vivo. *Proc Natl Acad Sci* **91:** 10340–10344.
Kerppola TK. 2008. Bimolecular fluorescence complementation (BiFC) analysis as a probe of protein interactions in living cells. *Annu Rev Biophys* **37:** 465–487.
Kerscher O, Felberbaum R, Hochstrasser M. 2006. Modification of proteins by ubiquitin and ubiquitin-like proteins. *Annu Rev Cell Dev Biol* **22:** 159–180.
Krogan NJ, Cagney G, Yu H, Zhong G, Guo X, Ignatchenko A, Li J, Pu S, Datta N, Tikuisis AP, et al. 2006. Global landscape of protein complexes in the yeast *Saccharomyces cerevisiae*. *Nature* **440:** 637–643.
Li SJ, Hochstrasser M. 1999. A new protease required for cell-cycle progression in yeast. *Nature* **398:** 246–251.
Li SJ, Hochstrasser M. 2000. The yeast *ULP2* (*SMT4*) gene encodes a novel protease specific for the ubiquitin-like Smt3 protein. *Mol Cell Biol* **20:** 2367–2377.
Makhnevych T, Sydorskyy Y, Xin XF, Srikumar T, Vizeacoumar FJ, Jerarn SM, Li ZJ, Bahr S, Andrews BJ, Boone C, et al. 2009. Global map of SUMO function revealed by protein-protein interaction and genetic networks. *Mol Cell* **33:** 124–135.
Panse VG, Hardeland U, Werner T, Kuster B, Hurt E. 2004. A proteome-wide approach identifies sumoylated substrate proteins in yeast. *J Biol Chem* **279:** 41346–41351.
Paulmurugan R, Gambhir SS. 2003. Monitoring protein-protein interactions using split synthetic renilla luciferase protein-fragment-assisted complementation. *Anal Chem* **75:** 1584–1589.
Periasamy A, Day RN. 1999. Visualizing protein interactions in living cells using digitized GFP imaging and FRET microscopy. *Methods Cell Biol* **58:** 293–314.
Pollok BA, Heim R. 1999. Using GFP in FRET-based applications. *Trends Cell Biol* **9:** 57–60.
Remy I, Michnick SW. 1999. Clonal selection and in vivo quantitation of protein interactions with protein-fragment complementation assays. *Proc Natl Acad Sci* **96:** 5394–5399.
Rigaut G, Shevchenko A, Rutz B, Wilm M, Mann M, Seraphin B. 1999. A generic protein purification method for protein complex characterization and proteome exploration. *Nat Biotechnol* **17:** 1030–1032.
Schmidt C, Peng B, Li Z, Sclabas GM, Fujioka S, Niu J, Schmidt-Supprian M, Evans DB, Abbruzzese JL, Chiao PJ. 2003. Mechanisms of proinflammatory cytokine-induced biphasic NF-κB activation. *Mol Cell* **12:** 1287–1300.
Seufert W, Futcher B, Jentsch S. 1995. Role of a ubiquitin-conjugating enzyme in degradation of S- and M-phase cyclins. *Nature* **373:** 78–81.
Sherman F. 2002. Getting started with yeast. *Methods Enzymol* **350:** 3–41.
Song J, Durrin LK, Wilkinson TA, Krontiris TG, Chen Y. 2004. Identification of a SUMO-binding motif that recognizes SUMO-modified proteins. *Proc Natl Acad Sci* **101:** 14373–14378.
Sung MK, Huh WK. 2007. Bimolecular fluorescence complementation analysis system for in vivo detection of protein-protein interaction in *Saccharomyces cerevisiae*. *Yeast* **24:** 767–775.
Sung MK, Huh WK. 2010. In vivo quantification of protein-protein interactions in *Saccharomyces cerevisiae* using bimolecular fluorescence complementation assay. *J Microbiol Methods* **83:** 194–201.
Sung MK, Ha CW, Huh WK. 2008. A vector system for efficient and economical switching of C-terminal epitope tags in *Saccharomyces cerevisiae*. *Yeast* **25:** 301–311.
Tarassov K, Messier V, Landry CR, Radinovic S, Serna Molina MM, Shames I, Malitskaya Y, Vogel J, Bussey H, Michnick SW. 2008. An in vivo map of the yeast protein interactome. *Science* **320:** 1465–1470.
Uetz P, Giot L, Cagney G, Mansfield TA, Judson RS, Knight JR, Lockshon D, Narayan V, Srinivasan M, Pochart P, et al. 2000. A comprehensive analysis of protein-protein interactions in *Saccharomyces cerevisiae*. *Nature* **403:** 623–627.
Wehrman T, Kleaveland B, Her JH, Balint RF, Blau HM. 2002. Protein-protein interactions monitored in mammalian cells via complementation of β-lactamase enzyme fragments. *Proc Natl Acad Sci* **99:** 3469–3474.
Wohlschlegel JA, Johnson ES, Reed SI, Yates JR. 2004. Global analysis of protein sumoylation in *Saccharomyces cerevisiae*. *J Biol Chem* **279:** 45662–45668.
Wykoff DD, O'Shea EK. 2005. Identification of sumoylated proteins by systematic immunoprecipitation of the budding yeast proteome. *Mol Cell Proteomics* **4:** 73–83.
Zhou WD, Ryan JJ, Zhou HL. 2004. Global analyses of sumoylated proteins in *Saccharomyces cerevisiae*. Induction of protein sumoylation by cellular stresses. *J Biol Chem* **279:** 32262–32268.

Received August 22, 2012; accepted in revised form February 7, 2013.